Mon. Not. R. Astron. Soc. **000**, 000–000 (0000) Printed 1 February 2008 (MN LATEX style file v1.4)

Testing models of X–ray reflection from irradiated disks

C. Done[1] & S. Nayakshin[2,3]

[1] *Department of Physics, University of Durham, South Road, Durham, DH1 3LE, England; chris.done@durham.ac.uk*
[2] *USRA and LHEA, NASA/Goddard Space Flight Center, Greenbelt, MD20771, USA; serg@milkyway.gsfc.nasa.gov*
[3] *Max Planck Institut fur Astrophysik, Karl-Schwarzschild-Str. 1, Postfach 1317, D-85741 Garching, Germany*

1 February 2008

ABSTRACT

We model the reflected spectrum expected from localized magnetic flares above an ionised accretion disk. We concentrate on the case of very luminous magnetic flares above a standard accretion disk extending down to the last stable orbit, and use a simple parameterisation to allow for an X–ray driven wind. Full disk spectra including relativistic smearing are calculated. When fit with the constant density reflection models, these spectra give both a low reflected fraction and a small line width as seen in the hard spectra from Galactic Black Hole Binaries and Active Galactic Nuclei. We fit our calculated spectra to real data from the low/hard state of Nova Muscae and Cyg X–1 and show that these models give comparable χ^2 to those obtained from the constant density reflection models which implied a truncated disk. This explicitally demonstrates that the data are consistent with either magnetic flares above an ionized disk extending down to the last stable orbit around a black hole, or with non-ionized, truncated disks.

Key words: accretion, accretion disks —radiative transfer — line: formation — X-rays: general — radiation mechanisms: non-thermal

1 INTRODUCTION

X–ray reflection is *in principle* a sensitive diagnostic of the X–ray source geometry. The amount of reflection depends on the solid angle subtended by the optically thick material, (and also on the ionisation and elemental abundances in the reflector) while the amount of relativistic smearing of the reflected spectral features (especially the iron Kα line and edge) shows how far this material extends down into the gravitational potential (see the review by Fabian et al. 2000 and references therein). This is important as there is much current debate about the structure of the X–ray source. One of the possibilities discussed in the literature is magnetic reconnection above the disk (e.g. Galeev, Rosner & Vaiana 1979, Haardt, Maraschi & Ghisellini 1994) while another is the advection dominated accretion flows (e.g. Narayan & Yi 1995). These result in very different source geometries – in the advective flows the inner disk is truncated, being replaced by an X–ray hot plasma, while the magnetic reconnection models have a disk which extends down to the last stable orbit.

The reflected spectrum is generally calculated *assuming* a given density structure of the disk (generally constant) as a function of height, and with a constant ionisation state as a function of radius. Fits with these models to spectra from both Galactic Black Hole Candidates (GBHC) and some Active Galactic Nuclei (AGN) show overwhelmingly that the solid angle subtended by the disk is generally less than unity, and that the relativistic smearing is less than expected for a disk which extends down to the last stable orbit (Życki, Done & Smith 1997; 1998; 1999; Zdziarski, Lubiński & Smith 1999; Chiang et al., 2000; Done, Madejski & Życki 2000; Miller et al., 2001). They also show that the solid angle and amount of smearing are *correlated* with spectral index in the sense that harder spectra show a smaller amount of reflection ($\Omega/2\pi << 1$) and narrower line emission (Życki et al., 1999; Zdziarski et al., 1999; Gilfanov, Churazov & Revnivstev 1999; 2000; Lubiński & Zdziarski 2001). Ionisation of the reflected spectrum is only strongly present for steep spectrum sources.

This rules out the simplest version of the magnetic flare model unless the flares generate a mildly relativistic outflow away from the disk (Beloborodov 1999). However, such outflows need not be required if the modelled reflected spectra are systematically underestimating the amount of reflection present in the data. For example, if the inner disk is so highly ionised that even iron is completely stripped, then reflection produces no spectral features (e.g. Fabian et al., 2000 and references therein). However, the data require a fairly sharp transition between the extreme ionisation and mainly neutral material, so as not to produce an intermediate region of high ionization, where iron is mainly H– and He–like, which

produces huge and unmistakable spectral features which are *not* present in the data (Done & Życki 1999; Done et al., 2000; Young et al., 2001).

It has recently been realised that X–ray illumination *changes* the density structure of the disk. The X–ray heated material at the top can expand outwards, lowering its density and increasing its ionisation. Calculating the self consistent density (and hence ionization) structure is especially important as there is a thermal ionization instability which affects X–ray illuminated material in pressure balance, which can lead to a hot, extremely ionised skin forming on top of the rest of the cooler, denser, mainly neutral disk material (Field 1965; Krolik, McKee & Tarter 1981; Kallman & White 1989; Ko & Kallman 1994; Różańska & Czerny 1996; Nayakshin, Kazanas & Kallman 2000, hereafter NKK; Różańska & Czerny 2000; Nayakshin & Kallman 2001, hereafter NK; Ballantyne, Ross & Fabian 2001).

The existance of the thermal instability can cause a substantial underestimate of the amount of reflection present as measured by the fixed density reflection model spectra (NKK; NK). This is explicially shown by Done & Nayakshin (2001, hereafter DN) and Ballantyne et al., (2001) for reflection from a single radius in the disk. Here we extend the calculations of DN to build full disk reflection models for the case of magnetic flares. We give a simple parameterization of the one major uncertainty in these models, which is the strength of any sideways expansion of the X–ray heated material from underneath the flare (see §2). We first fit the calculated total spectra (incident spectrum plus reflection from a disk with self consistent density structure including the thermal instability) with the power law plus fixed density reflection models in §3. We then fit the new models to actual data in §4 and show for the first time that the magnetic flare models (in which the disk subtends a solid angle of 2π) can fit the observed apparently weak reflection/narrow line, flat spectrum GBHC rather well. However, with these models, the data *require* moderate outflow rates from the X–ray heated region. Future work should explicitly calculate this sideways expansion of material, so as to remove the one remaining free parameter from the simplest magnetic flare model.

2 REFLECTED SPECTRA

The code of NKK gives the reflected spectrum from an X–ray illuminated slab whose vertical structure is given initially by that of an accretion disk (Shakura & Sunyaev 1973) at radius, r, and dimensionless mass accretion rate, $\dot{m} = \eta \dot{M} c^2 / \mathrm{L_{Edd}} = \mathrm{L}/\mathrm{L_{Edd}}$ ($\mathrm{L_{Edd}}$ is the Eddington accretion rate, L is the disk bolometric luminosity, $\dot{M}$ is the mass accretion rate and $\eta = 0.06$ is the radiative efficiency of the standard disk in Newtonian limit), where a fraction f_{corona} of the energy liberated by this infalling material is dissipated in a corona rather than in the optically thick disk (Svensson & Zdziarski 1994). This also defines the soft flux $F_{\rm disk}$ at the top of the disk due to viscous dissipation underneath. There is also additional heating from the illuminating X–ray flux $F_{\rm x}$ with spectral shape $F_{\rm x}(E)$, which then changes the vertical structure since the heated upper layer can expand. The steady state density structure is calculated under the hydrostatic equilibrium assumption.

The reflected spectrum from a full disk is an integral of reflected spectra from different radii. In practice we compute spectrum for only 6 radii due to CPU time limitations: r = 3.5, 4.9, 7, 14, 35 and 105 Schwarzchild radii for the same $\dot{m}$ and X–ray spectral shape, with a given radial dependance of the X–ray illuminating flux which depends on the X–ray source geometry. If the X-ray source(s) are magnetic flares due to the MHD dynamo responsible for the viscosity (Balbus & Hawley 1991) then the X–ray flux might be expected to scale with the disk flux i.e. $F_x \propto F_{disk} \propto r^{-3}$ so that F_x/F_{disk} is constant. The spectra from different radii can then be convolved with the relativistic transfer functions (assuming a Schwarzchild metric, but not including light bending: Fabian et al. 1989), which yields the requisite full disk relativistically broadened spectra.

Given the four initial parameters ($\dot{m}$, f_{corona}, F_x/F_{disk}, and X–ray spectral shape), together with the assumption that $F_x \propto F_{disk}$, the reflected spectra from magnetic flares should be completely determined for a given inclination angle. However, the assumption of hydrostatic equilibrium is *not* entirely justified because a local outflow is formed (NKK, NK). Hydrostatic balance predicts that the vertical scale height for a skin of temperature T is $H_s \sim (4kTR^3/GMm_p)^{1/2}$. Compare this with the standard disk vertical pressure scale height, H, using equations of Svensson & Zdziarski (1994):

$$\left(\frac{H_s}{H}\right)^2 = 2.5\times10^{-3} T_7 \left(\frac{\dot{m}(1-f_{corona})}{0.01}\right)^{-2} r^3 J(r)^{-2}\,, \quad (1)$$

where T_7 is the skin's temperature in units of 10^7 Kelvin, $\dot{m}$ is the dimensionless accretion rate, $r \equiv Rc^2/2GM$, and $J(r) = 1 - \sqrt{3/r}$. At radius $r = 6$, for example, this ratio becomes

$$\left(\frac{H_s}{H}\right)^2 = 6.5\, T_7 \left(\frac{\dot{m}(1-f_{corona})}{0.01}\right)^{-2} . \quad (2)$$

For Cyg X-1, $\dot{m}(1-f)$ is likely to be less than 0.01, and $T_7 \gtrsim$ few for hard X-ray spectra. Now, magnetic flares are likely to have height not much larger than $\sim H$ (Nayakshin & Kazanas 2001b) above the disk. Hence, the hydrostatic balance condition predicts that the skin can extend to height $H_s \gg H$, i.e., completely surround the X-ray source. This is inconsistent with the explicit assumption of the NKK code that X-rays are incident on the top of the skin at a given angle (equivalent to the source located at infinity from the disk).

In addition, when the X-ray source is engulfed by the highly photo-ionized skin, there is a large radiation pressure force directed away from the X-ray source. The gas expands upwards (away from the disk) and sideways (along the disk) due to the combination of thermal pressure and radiation pressure. The gas is moved on distances $H_s \gg H$ before the radiation force and illumination decreases so that the gas can both cool and fall back onto the disk. Note that the material *cannot* escape to infinity as it is gravitationally bound – the escape temperature from the inner accretion disk is $T \sim 10^{11}$ K (Begelman, McKee & Shields 1983). Note also that "local" winds do not occur for other than the magnetic flare models (see, e.g., NKK; NK, §4.1), where the hydrostatic balance assumption should be a good approximation.

NKK approximated the effects of this local outflow by

introducing a "gravity parameter" $A = \mathcal{F}_g/\mathcal{F}_{rad}$, which is the ratio of the vertical component of the gravitational force at the top of the disk, $\mathcal{F}_g = GMH\rho/R^3$, to the radiation pressure force, $\mathcal{F}_{rad} = F_{\rm x}\sigma_t n_e/c$. For a given $F_{\rm x}$, $\dot{m}$ and f_{corona}, the gravity parameter is uniquely determined. However, when the wind is present, hydrostatic balance does not apply as we discussed above. Therefore, NKK and NK allowed A to be a free parameter (even when $F_{\rm x}$ is fixed) to account for the poorly constrained strength of the wind. The Thomson thickness of the skin, τ_s, should always be lower if the wind is present compared with the values predicted by hydrostatic balance. By increasing the gravity parameter artificially, one also obtains smaller values of τ_s, hence qualitatively one can account for the wind by making A larger than its true value.

Here, instead of artificially increasing the gravity parameter, A, we try to develop a simple approximation to a local wind that should place us in approximately the correct part of parameter space. In particular, we write

$$\frac{\partial p}{\partial z} = -\frac{p}{\lambda}\,. \qquad (3)$$

where p is the gas pressure, and λ is the characteristic scale on which the gas pressure is decreasing. If hydrostatic balance assumption were appropriate, this scale would be the usual thermal pressure scale height (e.g., see λ as defined in Nayakshin 2000). Here the geometry leads us to consider the pressure changing on scales of order the height of the flare, which is of order H (Nayakshin & Kazanas 2001b). The coefficient of proportionality can only be found in a full scale 2 or 3-D calculation of this problem. Simple estimates show it can depend on the ratio of the X-ray and disk fluxes, $F_{\rm x}/F_{\rm disk}$, the Thomson thickness of the skin, disk accretion rate, etc. Therefore, we introduce a free dimensionless "wind parameter", Λ, to describe this uncertainty: $\lambda \equiv \Lambda H$.

Simple estimates show that $\Lambda \sim 1$ is appropriate to a thermally driven wind when the gas density decreases significantly at the distance $\sim H$ of the flare location. The case of small Λ corresponds to supersonic outflows, $v \gg c_s$ (c_s is the sound speed), when $\lambda \sim Hc_s/v$. We will vary Λ below and study its influence on the reflected spectra.

Summarizing, we use equation (3), together with $\lambda = \Lambda H$, to replace the hydrostatic balance condition in the NKK code (eq. 19 in NKK). The lower boundary conditions – continuity in the gas density and $T = T_{\rm eff}$ remain the same. The code then directly computes the density structure of the X–ray irradiated disk including the effects of this outflow, so this is clearly an improvement on the previous description which used hydrostatic balance with the *ad hoc* gravity parameter, A. In terms of gas temperature profiles, the results are not appreciably different than those using A in that the nearly discontinuous transition between the hot and cold phases is still present. However, the advantage of the new approach is that we hope (3) automatically puts us in the roughly the correct parameter space for real magnetic flares.

3 SIMULATED SPECTRA

We simulate spectra over a range of expected parameters for the hard X–ray spectra seen from GBHC and AGN. Plainly the spectral index of the incident power law influences the results, so we test two values of the index: $\Gamma = 1.6$ and $\Gamma = 1.8$. The power law is assumed to extend out to 200 keV, and then have an abrupt cutoff. This is a better model of a Compton scattered spectrum below ~ 80 keV than the very gradual rollover produced by an exponential cutoff. Observations seem to indicate $f_{corona} \sim 0.8$, so we fix this in all simulations. We assume an underlying disk accretion rate of $\dot{m} = 0.03$ (this contrasts with the $\dot{m} = 10^{-3}$ assumed in paper 1) onto a super–massive black hole of $10^8 {\rm M}_\odot$. The large black hole mass means that we avoid disk photons potentially contributing to the observed bandpass, and more importantly numerically we avoid the very high densities in GBHC disks for which the atomic data and codes are not reliable. XSTAR 2.0 (Kallman & Bautista 2001) has the highest density range of current photo–ionisation codes, but even this breaks down at $\sim 10^{18}$ cm^{-3}, whereas the GBHC disks can have densities of $\sim 10^{20}$ cm^{-3} in the ionised skin, and 10^{22} cm^{-3} in deeper layers. It is simply not possible to calculate the ion populations in X–ray illuminated GBHC disks with current codes. We use the AGN reflected spectra as the best current approximation to those from GBHC, but we caution that the GBHC ion populations can be different from those given here.

To obtain flat spectra, i.e. $\Gamma < 2$, requires that the power dissipated in heating the electrons in the flare is much larger than the seed photon luminosity available for Compton scattering (e.g., Pietrini & Krolik 1995; Stern et al. 1995, Poutanen & Svensson 1996). Further, in order to produce reflected spectra with little He-like Fe contribution, one needs the skin to be essentially completely ionized. Within a factor of few, both of these conditions require the X-ray flux incident on the disk surface near flares footpoints to be much larger than the disk flux, i.e., $F_{\rm x} \gg F_{\rm disk}$. We thus decided to test values of $F_{\rm x}/F_{\rm disk}$ anywhere between $\sim 10-100$, and we choose a grid of $F_{\rm x}/F_{\rm disk} = 10, 30, 100$. We also choose a grid for the wind parameter of $\Lambda = 0.03, 0.1, 0.3$ and 1.

This results in 24 model spectra of reflection from a disk which extends down to the last stable orbit. We simulate these spectra through the RXTE PCA response, assuming a flux of $\sim 10^{-8}$ ergs cm^{-2} s^{-1} and a 1ks exposure (i.e. comparable to a single PCA orbit of a bright GBHC). The resulting 3–20 keV spectra have systematic errors of 0.5 per cent added in quadrature to the (negligible) statistical errors since it is sadly unlikely that any satellite will be calibrated to better accuracy than this. These spectra are fit using the fixed density ionization models without relativistic smearing (`pexriv`: Magdziarz & Zdziarski 1995), with a separate narrow (intrinsic width fixed at 0.1 keV) Gaussian line of free normalization, and energy (except that this latter is constrained to be between 5.5 and 7.5 keV, as expected for iron with some shifts allowed for Doppler and gravitational effects). All the fits were statistically acceptable ($\chi^2_\nu = 0.6 - 1.2$ for 38 degrees of freedom) and gave a derived ionization consistent with mostly neutral material except for the case with $F_{\rm x}/F_{\rm disk} = 100$, $\Lambda = 1$. This extreme illumination with slow wind results in a large optical depth in the hot layer (≥ 1), so the observed reflected spectrum comes from the lower temperature material in the hot layer rather than the cool material underlying the skin. This gives rise to a clearly ionised reflected signature, so these data are not shown in the following plots.

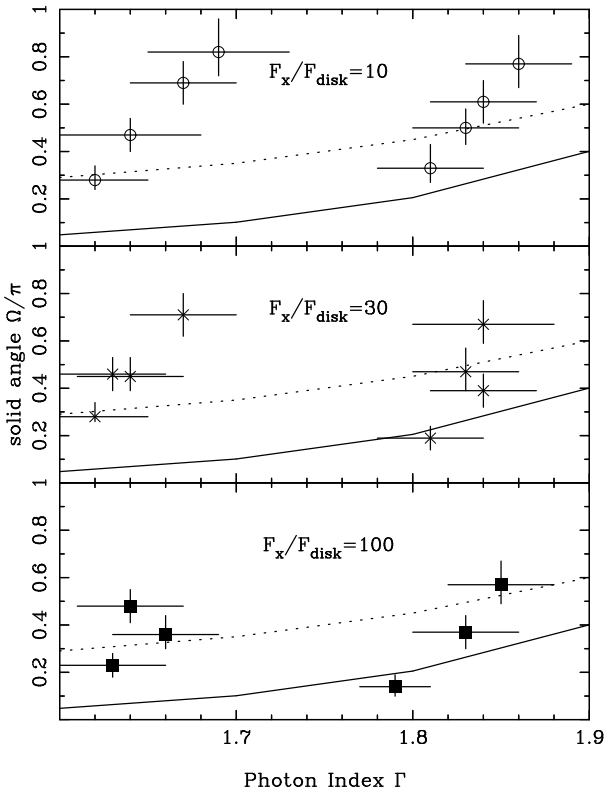

Figure 1. Derived values of spectral index and reflected fraction for simulated RXTE datafiles made from the illuminated disk models, fit with the `pexriv` constant density reflection model. The models are calculated for $F_x/F_{disk} = 10$ (large circles; upper panel), 30 (crosses; middle panel), and 100 (squares; lower panel), each with wind parameter $\Lambda = 0.03, 0.1, 0.3$ and 1 (except for $F_x/F_{disk} = 100$ where $\Lambda = 0.03, 0.1$ and 0.3). Stronger winds (small Λ) have smaller optical depth in the extremely ionized skin, and so have larger reflected fractions. The solid line in each panel is the observed index–reflection correlation of Zdziarski et al. (1999), while the dotted line is that observed for GBHC (Gilfanov et al., 2000).

Figure 1 shows the resulting derived photon spectral index, Γ, and solid angle, $\Omega/2\pi$ for each different $F_{\rm x}/F_{\rm disk}$. For a given spectral index, the optical depth of the ionized layer is larger for higher $F_{\rm x}/F_{\rm disk}$, and for slower winds. The solid line shows the overlaid $\Gamma - \Omega/2\pi$ correlation derived by Zdziarski et al., (1999) for a sample of AGN and GBHC, while the dotted line shows that derived from GBHC by Gilfanov et al., (2000). Clearly, the simulated spectra can match the observed correlations only if the wind strength and $F_{\rm x}/F_{\rm disk}$ are varied in the "right way". Unfortunately values of these parameters depend crucially on the (currently unknown) physics of magnetic flares, e.g. on how the height of the flare might evolve as a function of mass accretion rate, so it is hard to see whether these parameters will indeed cooperate to produce the observed correlations.

We get similar results (see Figure 2) in terms of derived spectral index and reflected fraction when using the reflection code developed by Życki et al., (1999). This code has the iron line intensity and energy tied self–consistently to the continuum reflection, and then both line and reflected continuum are smeared by relativistic effects. Again the models fit the simulated data well, and imply a low ionization state of the reflecting material, but the difference now is that the spectral broadening of the line and reflected edge can be constrained. Figure 2b shows the amount of smearing (in units of gravitational radii $R_{\rm g} = GM/c^2$ rather than Schwarzchild radii, $R_s = 2R_{\rm g}$). In general a higher optical depth (slower wind and higher $F_{\rm x}/F_{\rm disk}$) gives less smearing, but *none* of the spectra show the extremely smeared and skewed components which are associated with the last stable orbit around the black hole.

Clearly the resolution from proportional counters leaves much to be desired. To investigate the smearing further we simulated the model spectra through the ASCA GIS response, assuming a mean 2–10 keV flux of $\sim 10^{-8}$ ergs cm^{-2} s^{-1}, and a 20 ks exposure (as typical for the Cyg X–1 observations: Ebisawa et al., 1996). We fit these spectra with the relativistically smeared reprocessed spectral model of Życki et al., (1999) over the 4–10 keV band (for comparison with the GIS Cyg X–1 data of Done & Życki 1999). Again all the fits are adequate ($\chi^2_\nu = 0.75 - 1.25$ for 79 degrees of freedom) with the reflected spectrum ionisation indicating mainly neutral material. Figure 3a shows the resulting derived spectral index and solid angle, showing that curvature in the data can be more easily matched in the narrower bandpass data by a somewhat steeper spectral index and correspondingly higher reflected fraction. Figure 3b shows the resulting inner disk radii. Again the reflected spectral features are *never* as broad as expected if the reflector were a constant density disk extending down to the last stable orbit in a Schwarzchild geometry.

This latter fact is somewhat surprizing given that the Thomson depth of the skin is quite low, $\tau_s \sim 0.1$, for the strongest wind models. Experimenting with fits, we found

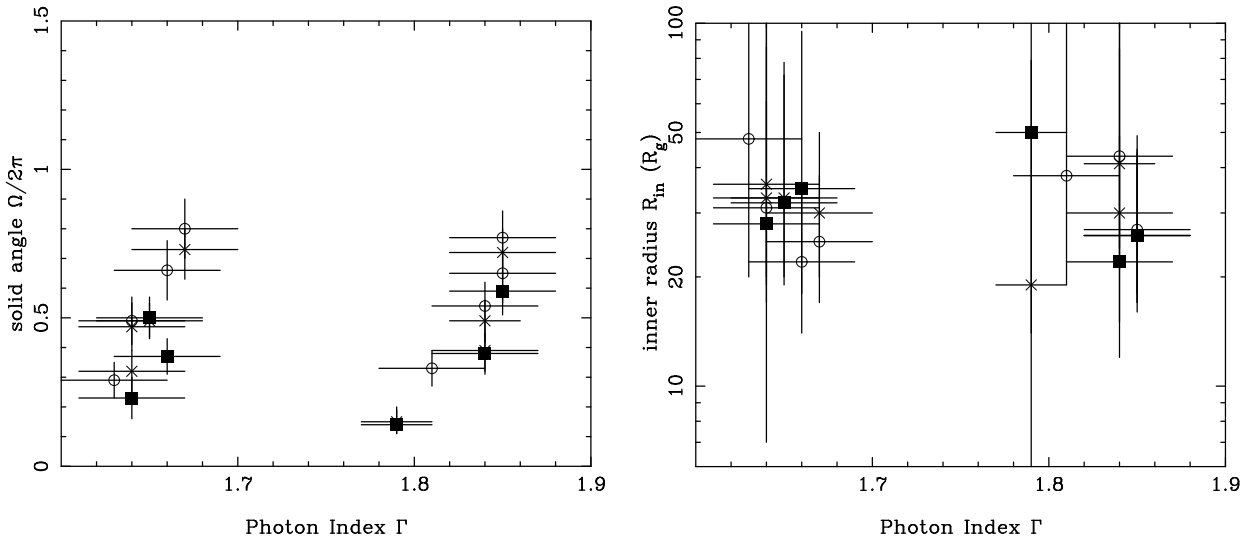

Figure 2. (a) Derived values of spectral index and reflected fraction from the simulated XTE datafiles shown in Figure 1 but fit with constant density reflection models of Życki et al., (1999). These include the self–consistently calculated iron emission lines for a given reflected continuum, and relativistically smear both line and continua together. The symbols are the same as for Figure 1. It is again clear that the optical depth of the extremely ionized skin is the major factor which determines the properties of the observed spectrum, but this is dependent on the (currently unknown) wind strength. (b) Derived values of the inner disk radius in units of $R_{\rm g} = GM/c^2$ obtained from the fits in (a), plotted against the spectral index. While the RXTE resolution is fairly poor, the line is *never* as broad as expected if the reflector were a constant density disk extending down to the last stable orbit in a Schwarzchild geometry ($\equiv 6R_{\rm g}$).

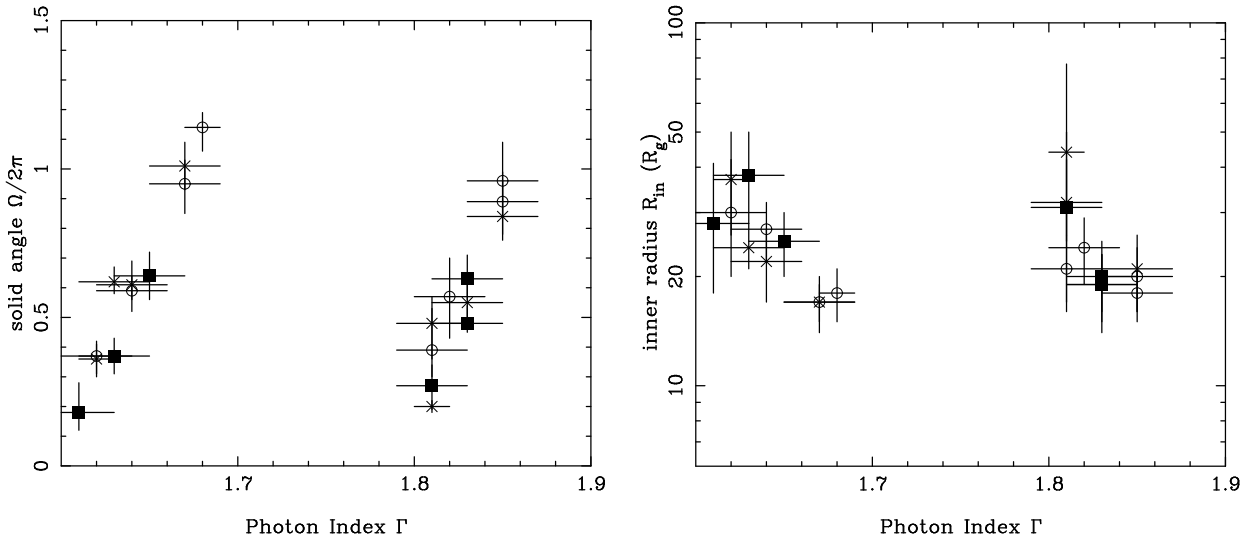

Figure 3. As for Figure 2a and b, but with fits to simulated ASCA GIS datafiles. (b) The moderate resolution of the GIS detectors gives better constraints on the amount of relativistic smearing than those obtained from the RXTE simulations (figure 2b). Plainly the ionized skin suppresses the line emission from the innermost regions, leading to derived disk radii which are *always* larger than 3 Schwarzchild radii ($\equiv 6R_{\rm g}$).

that the main reason that the inner disk radius is larger in the fits than in the actual models is that the broad redshifted wing of the Fe Kα line gets confused with the incident power-law. Indeed, the inferred value of Γ differs from the actual one by as much as 0.1 for the strongest wind cases.

4 REAL DATA

Plainly these model spectra bear a close resemblance to the data in terms of the properties of the reflected spectrum. The next step is to fit such models to real data. As a first attempt at this we have taken the tabulated spectra used above and incorporated them into the XSPEC spectral fitting package (Arnaud 1996) as a local model. With this approach the only true free parameter is the normalisation of the reflected spectrum, but we have approximated the change made by small variations of spectral slope ($\Delta\Gamma \leq 0.1$ by multiplying the models calculated for a given spectral index Γ_0 by the factor $E^{\Gamma-\Gamma_0}$. We have models tabulated for $\Gamma_0 = 1.6$ and 1.8, and these give *reflected* spectrum for $\Gamma = 1.7$ which

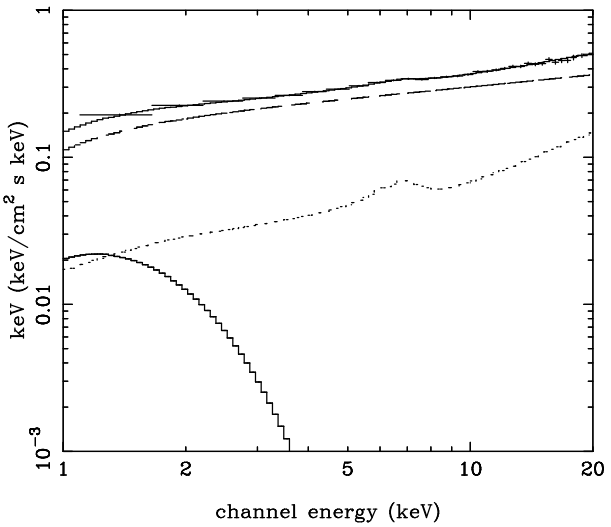

Figure 4. Data from the transient black hole Nova Musca taken on July 23 1991 when the source showed a classic low state spectrum. The data are well described by the complex ionization reflection models presented here. The dashed line shows the incident power law (which is absorbed at low energies by the interstellar column of 1.6×10^{21} cm^{-2}) while the dotted line shows its reflection from a disk with a completely ionized skin ($\Lambda = 0.3$, $F_x/F_{disk} = 10$, $i = 63°$). The lower solid line shows the contribution from the disk blackbody spectrum.

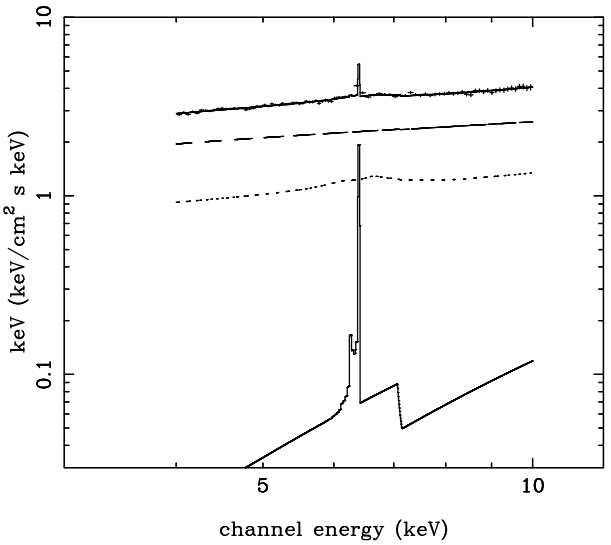

Figure 5. ASCA GIS data for Cyg X–1 fit to the complex ionization reflection models presented here. The dashed line shows the incident power law while the dotted line shows its reflection from a disk with a completely ionized skin ($\Lambda = 0.3$, $F_x/F_{disk} = 100$, $i = 49°$). The lower solid line shows the unsmeared, neutral reflection from the companion star/outer disk.

are consistent to within 5% in the 2–20 keV band, so the total spectra for $\Gamma = 1.7$ derived from $\Gamma_0 = 1.6$ and 1.8 are consistent to within 2 %.

The first test is for broad band data from GINGA. A classic GBHC low state spectrum is that of Nova Muscae on July 23rd 1991. The constant density (single ionization parameter) reflection models give a best fit of $\chi^2 = 15.3/24$ for a model consisting of a disk blackbody, together with a power law and its relativistic reflection component (inclination fixed at 60°) with $\Gamma = 1.72 \pm 0.02$, $\Omega/2\pi = 0.24^{+0.11}_{-0.08}$, $R_{\rm in} = 50^{+\infty}_{-35} R_{\rm g}$, all absorbed by a (fixed) column of $N_H = 1.6 \times 10^{21}$ cm^{-2} (Życki et al., 1998). We replace the power law and its relativistic reflection by the model spectra used above (incident flux plus its reflection from the complex ionization structure of the disk) for $\Gamma_0 = 1.8$ and step over all tabulated values of F_x/F_{disk} and Λ. The best fit is shown in Figure 4, giving $\chi^2_\nu = 18.5/25$ for $F_x/F_{disk} = 10, \Lambda = 0.3$. Plainly low resolution, broad band data where the reflected spectrum appears to have much lower normalisation and smearing than expected for a disk around a black hole can be well fit by these model spectra which have the disk subtending a solid angle of unity and extending down to the last stable orbit.

A higher resolution spectrum gives a better test of the relativistic smearing constraints. We use the ASCA GIS 6 data from Cyg X–1 of Ebisawa et al., (1996), as analysed by

Done & Życki (1999) in the 4–10 keV range. We step over inclinations from $56^\circ - 31^\circ$ as the inclination of the Cyg X–1 system is not well known, and include a narrow, neutral reflected component (solar abundance, inclination of 60°, with line normalisation and energy tied to the reflected continuum) to account for the contribution to the reflected spectrum from the companion star. The interstellar column is fixed at 6×10^{21} cm^{-2}. This gives a best fit of $\chi^2_\nu = 83.8/79$ for $\Lambda = 0.3, F_x/F_{disk} = 100, i = 49^\circ$, shown in Figure 5. There are many other solutions within $\Delta\chi^2 = 6.25$ (90 per cent confidence for 3 parameters), although none of these allow the strongest wind with $\Lambda = 0.03$. The quality of the fit is plainly comparable to that of the constant ionization models of Done & Życki (1999), who obtained $\chi^2_\nu = 81.4/79$, $\Omega/2\pi = 0.10^{+0.17}_{-0.09}$ and $R_{\rm in} = 18^{+30}_{-12} R_{\rm g}$. Thus even high resolution data which appears to show much less reflection and (marginally) smearing from the accretion disk than expected can be fit with the models where the ionization instability gives rise to a completely ionized skin on the disk overlying more neutral material.

5 CONCLUSIONS

We use a modified version of the code of NKK and NK to calculate the vertical structure of an X–ray illuminated disk at a given radius, and then sum these spectra over all radii, with appropriate relativistic smearing, to get the full disk reflected spectra expected from magnetic flares. However, the reflected spectra are *not* uniquely determined as the local intense illumination expected from magnetic flares can drive outflows from the illuminated region, lowering the optical depth of the ionized skin. We approximate the effects of this with a free parameter Λ (equation 3). We simulate full disk reflected spectra for a grid of different $F_x/F_{disk} = 10, 30$ and 100, with spectral index $\Gamma = 1.6, 1.8$ and with $\Lambda = 0.03, 0.1, 0.3$ and 1.

We simulate each total spectrum (illuminating power law plus full disk reflection) through the low resolution RXTE and moderate resolution ASCA GIS response and fit these with the constant density (single ionization state) `pexriv` models. The ionized skin reduces the derived $\Omega/2\pi$ for a given spectral index, and also reduces the amount of relativistic smearing observed as the ionized skin depth is at its maximum in the inner disk.

The resemblance of the (low–to moderate wind velocity) simulated spectra to observations of low–state GBHC and AGN is striking. The models have the disk sub–tending a solid angle of 2π and extending down to the last stable orbit, but the vertical ionization structure can mask the reflected signature especially from the inner disk. When such spectra are fit with the constant density reflection models then the derived solid angle and iron line width *appear* to imply that the disk subtends a small solid angle and has a large inner disk radius. These simulations of a full disk confirm the conclusions of DN and Ballantyne et al., 2001, drawn from local (single radius) models that the observations of a small solid angle and line width do not necessarily rule out static magnetic flares above an untruncated disk.

We show for the first time that these magnetic flare models can fit real data. Both low resolution (GINGA data from the low/hard state of Nova Muscae, Życki et al., 1998) and moderate resolution (ASCA GIS data from the low/hard state of Cyg X–1, Done & Życki 1999) can be fit with these full disk models. The χ^2 for these fits is comparable to that obtained from the constant density reflection models which implied a truncated disk. Thus the data can be consistent with *all* the currently proposed X–ray production mechanisms – either simple (static) magnetic flares, or with outflowing plasma from a magnetic flare, or with a truncated disk/inner X–ray hot (advective) flow.

To make progress we clearly need more sophisticated models of the reflected spectra. It is probable that the primary reason that all these different models can fit the data is because of the current freedom in the values of model parameters (e.g., Λ for the wind from magnetic flares: the relativistic outflow velocity in the plasma ejection models: Beloborodov 1999; the transition radius in the advective flow models: Esin, McClintock & Narayan 1997). In particular, the magnetic flare models should be improved via an explicit calculation of the X–ray induced wind. This may limit the range of possible Λ for a given $F_{\rm x}/F_{\rm disk}$, ruling some models out. For the cold outer disk plus inner hot flow models, the next step is to include the presence of the skin on the cold disk – the physics of the thermal ionization instability applies to all configurations of the disk. Another modelling issue which needs to be addressed is the current inability of the atomic codes to handle the high densities required to properly model the GBHC disks.

We also need better data, especially observations which extend over a wider bandpass. Including the higher energy spectra beyond 20 keV may start to break the degeneracy between the different model spectra (DN), while simultaneous lower energy data can constrain the seed photon flux. Another possible way to distinguish between the models is to study their variability behaviour. The ionised skin of the disk can respond to changes in the illuminating flux on a timescale of the order of the Keplerian rotation time scale. This time scale is longer than the light crossing time at the same radius (Nayakshin & Kazanas 2001a). In other words, a highly variable light curve may produce reflected spectra that are different from the steady-state models (studied in this paper), which then could be used to differentiate between the models. Finally, and perhaps most convincingly, Fe Kα line reverberation studies should present a variety of constraints on the models (Reynolds 2000, Revnivtsev et al. 1999). Recently, Nayakshin & Kazanas (2001b) showed that time-resolved Fe Kα line from a single magnetic flare is *narrow* but is moving across the $\sim 4 - 8$ keV band. This prediction is completely different from the instantaneous line profile expected in a central source or lamppost–like geometry (e.g., Young & Reynolds 2000, Ruszkowski 2000), and one can hence hope that that will be the definitive test of the accretion flow geometry.

6 ACKNOWLEDGEMENTS

SN acknowledges support from NRC Research Associateship. The authors thank Demos Kazanas and Piotr Życki for useful discussions. We are indebted to the anonymous referee for pointing out a very serious typographical error in the equation (3).

REFERENCES

Arnaud K. A., 1996, Astronomical Data Analysis Software and Systems V, eds. Jacoby G. and Barnes J., p17, ASP Conf. Series volume 101.

Balbus S. A., Hawley J. F., 1991, ApJ, 376, 214

Ballantyne D., Ross R., Fabian A. C., 2001, MNRAS, in press

Begelman M. C., McKee C., Shields G., 1983, ApJ, 271, 70

Beloborodov A. M. 1999, ApJ, 510, L123

Chiang J., Reynolds C. S., Blaes O. M., Nowak M. A., Murray N., Madejski G., Marshall H. L., Magdziarz P., 2000, ApJ, 528, 292

Done C., Madejski G. M., Życki P. T., 2000, ApJ, 536, 213

Done C., Nayakshin S., 2001, ApJ, 546, 419 (DN)

Done C., Życki P. T., 1999, MNRAS, 305, 457

Ebisawa K., Ueda Y., Inoue H., Tanaka Y., White, N. E., 1996, ApJ, 467, 419

Esin A. A., McClintock J. E., Narayan R., 1997, ApJ, 489, 865

Fabian A. C., Rees M. J., Stella L., & White N. E., 1989, MNRAS, 238, 729

Fabian A. C., Iwasawa K., Reynolds C. S., Young A., 2000, PASP, 112, 1145

Field G. B., 1965, ApJ, 142, 431

Galeev A. A., Rosner R., Vaiana G. S., 1979, ApJ, 229, 318

Gilfanov M., Churazov E., Revnivtsev M., 1999, A&A, 352, 182

Gilfanov M., Churazov E., Revnivtsev M., 2000, 5th CAS/MPG Workshop on High Energy Astrophysics (astro-ph/0002415)

Haardt F., Maraschi L., Ghisellini G., 1994, ApJ, 432, 95

Kallman T. R., Bautista M., 2001, ApJS, 133, 221

Kallman T. R., White N. E., 1989, ApJ, 341, 955

Ko Y.–K., Kallman T. R., 1994, ApJ, 431, 273

Krolik J. H., McKee C. F., Tarter C. B., 1981, ApJ, 249, 422

Lubiński P., Zdziarski A. A., 2001, MNRAS, 323, L37

Magdziarz P., Zdziarski A. A., 1995, MNRAS, 273, 837

Miller J. M., Fox D. W., Di Matteo T., Wijnands R., Belloni T., Pooley D., Kouveliotou C., Lewin W. H. G., 2001, ApJ, 546, 1055

Narayan R., Yi I., 1995, ApJ, 444, 231

Nayakshin S. 2000, ApJ, 534, 718.

Nayakshin S., & Kallman T. R., 2001, ApJ, 546, 406 (NK)

Nayakshin S., & Kazanas D., 2001a, ApJ, 553, L141

Nayakshin S., & Kazanas D., 2001b, submitted to ApJ

Nayakshin S., Kazanas D., & Kallman T. R., 2000, ApJ, 537, 833 (NKK)

Pietrini P., Krolik J. H., 1995, ApJ, 447, 526

Poutanen J., Svensson R., 1996, ApJ, 470, 249

Revnivtsev M., Gilfanov M., & Churazov E., 1999, A&A, 347, L23

Reynolds C. S., 2000, ApJ, 533, 811

Różańska A., Czerny B., 1996, AcA, 46, 233

Różańska A., Czerny B., 2000, A&A, 360, 1170

Ruszkowski M., 2000, MNRAS, 315, 1

Shakura N. I., Sunyaev R. A., 1973, A&A, 24, 337

Stern B. E., Poutanen J., Svensson R., Sikora M., Begelman M. C., 1995, ApJ, 449, 13

Svensson R., Zdziarski A. A., 1994, ApJ, 436, 599

Young A., Reynolds C. S., 2000, ApJ, 529, 101

Young A., Fabian A. C., Ross R., Tanaka Y., 2001, MNRAS, in press

Zdziarski A. A., Lubiński P., Smith D. A., 1999, MNRAS, 303, 11

Życki P. T., Done C., Smith D. A., 1997, ApJ, 488, L113

Życki P. T., Done C., Smith D. A., 1998, ApJ, 496, L25

Życki P. T., Done C., Smith D. A., 1999, MNRAS, 305, 231